ORIGINAL ARTICLE

Effectiveness of Sequential Pre-treatment and Application of High-porosity Hybrid Fly Ash Geopolymer/alginate Adsorbent for the Treatment of Batik Wastewater

Siti Mazatul Azwa Saiyed Mohd Nurddin[1], Suriati Sufian[*2], Zakaria Man[1], Nurul Ekmi Rabat[1], Nazwin Ahmad[2]

[1]*Department of Chemical Engineering, Universiti Teknologi PETRONAS, 31260 Bandar Seri Iskandar, Perak, Malaysia*

[2] *Mineral Research Centre, Jalan Sultan Azlan Shah, 31400 Ipoh, Perak, Malaysia*

ABSTRACT: In this work, hybrid fly ash geopolymer / alginate spheres (GSA) were produced and used as an effective and economical adsorbent in a treatment of batik wastewater. A preparation of GSA adsorbent involved a facile method where the fly ash (FA) based geopolymer was entrapped into sodium alginate (SA) followed by cross-linking of Ca^{2+} and SA. In additional to that, natural egg white was utilized as a foaming agent. Characterization of the GSA adsorbent strongly confirmed the formation of hybrid spheres that composed of geopolymer and alginate with extremely porous microstructure with porosity of 87.64%. Surface area, average pore diameter and pore volume was 12.874 m^2 g^{-1}, 3.3110 nm and 0.1684 cm^3 g^{-1}, respectively. Prior to the adsorption process, the batik wastewater was pre-treated using high concentration acid hydrofluoric (HF) and magnesium oxide (MgO). The optimum acidification pre-treatment at pH=3 removed ~ 93% of chemical oxygen demand (COD). In the subsequent stage, the highest percentage of COD removal was ~27% by utilizing 1500 mg L^{-1} of MgO powder. In the final stage, different dosages of GSA adsorbent was used in order to treat the remaining COD and resulted in as maximum as ~67% of the COD removal. According to the finding, the sequential pre-treatment and application of high-porosity hybrid GSA adsorbent offered a great potential to be implemented as an economical and effective batik wastewater treatment.

INTRODUCTION

Textile industry is one of the industries that use large quantities of dyes, chemicals and water at every stage of the production [1-3]. However, the resultant waste was mostly released to the ecosystem without a proper treatment [4]. It is estimated that around 10 – 15% of textile dyes do not bind to the fabric during the dyeing process and has been discharged to the environment causing numerous environmental issues such as water pollution that lead to disturbance in aquatic life[5]. According to the current scenario, a proper wastewater treatment for coloured effluents should be conducted prior to discharge.

One of the oldest cottage textiles in Malaysia is batik industry which are scattered throughout Kelantan and Terengganu. Most of the batik productions are run in a small family based set-up that do not conduct any wastewater treatment. Furthermore, a proper wastewater treatment is also difficult to be established as the locations are considerably sporadic [3]. The main problem that is related to batik wastewater besides

involving large volumes of water is the contents of waxes, dyes and fixing agents such as silicate which resulting in high pH, COD, total suspended solids (TSS) and heavy metals[6]. The presence of waxes and various chemicals in the effluents have made it difficult to be treated due to the complexity of the pollutants [7-9]. Commonly, there are three major sequential steps involves in the batik processing namely soaking, boiling and rinsing which each has their own pollutants. The boiling and soaking steps of the batik processing contain high amounts of COD, silicate and heavy metals. Therefore, an appropriate technique is required to remediate the wastewater in compliance with the local standards and regulations before being released into the environment [9].

Recently, physical and chemical treatment is the most applied method for treating textile wastewater that commonly contain basic dyes, e.g. safranin, crystal violet, malachite green, and methylene blue[10] due to its low cost, simplicity of utilization, economical and effectiveness compared to biological treatment which is difficult to be implemented and required long retention time[11-13]. Moreover, this method is also not possible for treating wastewater that contains high heavy metal[14]. In particular, nano-filtration and reverse osmosis method can reclaim water and chemicals, but they are considerably expensive and have significant fouling problems. Furthermore, if the wastewater contains high salts from the dyeing process, the ultra filtration method cannot be used repeatedly [15]. Electro-kinetic coagulation method is also effective in wastewater treatment, but the major limiting factor of this method is it generates large amount of sludge and it consumes high processing energy [16]. Another feasible method that have been reported for treating colour effluents is photocatalysis[17-19]. As batik wastewater is not only containing dye thus, all of the aforementioned methods are not able to effectively treat batik wastewater. This condition is due to high contents of silica, wax and heavy metal which brings people to figure out for more effective, feasible and economical approach for treating the wastewater from batik process.

Activated carbon is the most common adsorbent that possesses high surface area and adsorption capacity; chemical inertness and is frequently used as the benchmark of adsorbent materials[20]. However, its widespread use is limited by the high production cost and microporous structure (< 2.0 nm) that does not allow the adsorption of bulky dye molecules and low recovery after usage due to its powder type adsorbent [12]. Therefore, there is a need for other adsorbents that are composed of inexpensive materials which can be attained from various available wastes which then isconverted into more attractive inorganic polymer known as geopolymer.

Geopolymers are aluminosilicate based polymer which is commonly derived from metakaolin, fly ash and granulated blast furnace slag (GBFS) that consist of polymeric silicon-oxygen-aluminium framework structures [21]. Currently, there are new sources of aluminosilicate materials including biomass fly ash[12], bottom ash[22], red mud[23], rice husk ash[11] and clays[24] which show good characteristics to be applied as geopolymer starting materials.

In this work, batik wastewater was subjected to a sequential pre-treatment prior to the adsorption by geopolymer/alginate adsorbent. This pre-treatment method consisted of an acidification step using concentrated hydrochloric acid (HCl) and a treatment using MgO powder. In the acidification step, the silicate polymerization was instigated by the concentrated HCl in which the resulting polymerized silicate was coordinated with the oxygenated groups of wax and the other major organic pollutants in the wastewater. In the next step, MgO powder was used to remove the remaining silicate, wax and heavy metal. In the final step, the geopolymer/alginate adsorbent was used to treat the organic fraction in the wastewater. The main objective of this study was to determine the effectiveness of geopolymer/alginate adsorbent in treating batik industry wastewater through the sequential pre-treatment that involved the acidification and treatment using MgO powder. Furthermore, the efficacy of each step of the pre-treatment was analyzed.

MATERIALS AND METHODS

Materials

The FA was obtained from a power station situated in Manjung, Malaysia and only particle size fraction below 45 µm was used in the preparation of the geopolymer

adsorbent. Sodium alginate (SA), calcium chloride (CaCl$_2$), sodium hydroxide (NaOH) and methylene blue (MB) were purchased from Sigma Aldrich and natural egg white was supplied by Nutri-plus, Malaysia. The preparation of all required solutions was carried out using deionized water. The batik wastewater used in this study was obtained from a small-scale batik factory located in Terengganu, Malaysia. The wastewater was collected from the soaking point of the batik processing and preserved at 6°C prior to a batch testing. The colour of the collected wastewater was dark blue. Concentrated HCl (37%) was purchased from R&M (Malaysia) and MgO powder (99%) was supplied by Sigma Aldrich, Malaysia.

Synthesis and characterization of geopolymer adsorbent

High-porosity geopolymer/alginate spheres (GSA) were prepared by cross-linking between calcium ion (Ca^{2+}) from CaCl$_2$ and SA which strengthened by geopolymer slurry and addition of egg white as the foaming agent. Geopolymer paste was firstly prepared by mixing the FA and NaOH with a mass ratio of fly ash to NaOH was 3:1. Subsequently, SA solution (2.0 wt%) was added into the geopolymer paste before 15 wt% egg white was mixed into the geopolymer paste while stirring. Finally, the slurry was dropwised into a CaCl$_2$ solution (2 wt%) and the formed spheres were kept in the solution for 24 h at room temperature. The 2-5 mm diameter spheres were drained, washed and cured at 60 °C for 24 h. Surface area and porosity analyser (Micrometrics ASAP 2020, ASAP, USA) was used to determine the surface properties of the GSA adsorbent. The phase analysis was performed using x-ray diffraction (XRD) (Bruker D8 Advance, Germany) and carried out at the diffraction angles of 10° to 70°C. Fourier transform infrared (FT-IR) spectroscopy (Perkin-Elmer Spectrum One Fourier Transform-Infrared Spectrometer, USA) analysis was conducted to analyse the functional groups and chemical bonding of the adsorbent at the range of 450-4000 cm^{-1}. The micromorphology and surface profile of the adsorbent was verified using field emission scanning electron microscopy (FESEM) (Carl Zeiss, Supra 55 VP Scanning Electron Microscope, Germany). For comparison study, unhybridized geopolymer adsorbent of the equivalent

composition was also evaluated by the same characterization.

Batik wastewater pre-treatment

Characterization of the untreated batik wastewater which included determination of chemical oxygen demand (COD), American Dye Manufacturers Instutite (ADMI) colour intensity, pH, total suspended solid (TSS) and turbidity was conducted before subjected to the sequential pre-treatment process. The pH of the batik wastewater was measured using a pH meter (Metler Toledo, USA). The COD analysis was performed using high range (20-1500 mg L^{-1}) COD reagent vial (HACH, USA) (Method 8000). 2 mL of the sample was pipetted into the COD reagent vial prior to place in the COD reactor (HACH, DRB200, USA) and heated at 150°C for 2 hrs. Then, it was cooled before subjected to analysis by colourimetric method performed by spectrophotometer (HACH, DR3900, USA). The reacted sample was represented by the appearance of green colour, which indicated the condition either the COD can be measured or the sample required to be diluted. The percentage of degradation was calculated by the following equation [14]:

$$\frac{C_o - C_t}{C_o} \ X \ 100\% \qquad (1)$$

Where,

C_t = COD or ADMI colour intensity for treated batik wastewater.

C_0 = initial COD or ADMI colour intensity of batik wastewater.

In TSS analysis, 40 mL batik wastewater was vacuum filtered with 0.45 μm-pore filter paper (Whatman, Japan) and the filter paper with the residue were oven dry at 105°C for 1 hr and the final weight was recorded. Prior to that, the same filter paper was dried in an oven for 1 hr at 105°C and cooled in a dessicator for 30 min. Then, the initial weight of the filter paper was recorded after the cooling process. The TSS of the batik wastewater was calculated as follows [25]:

TSS (mg L^{-1}) = [final weight (mg) − initial weight (mg)] / Volume of the batik wastewater   (2)

The turbidity analysis was performed using a turbidity meter (HACH 2100Q, USA) through a few quick

measurements. 20 mL of batik wastewater was placed in a sample cell and the average reading was recorded.

Batik wastewater pre-treatment and treatment by hybrid geopolymer / alginate adsorbent

The sequential pre-treatment process involved the acidification using concentrated HCl and pre-treatment using MgO powder as described by Birgani [14]. In the acidification, concentrated HCl was gradually added into 3 different beakers containing 1000 mL batik wastewater each until it reached pH 1, 2 or 3 under magnetic stirring at 100 rpm for approximately 30 min. The batik wastewater was vacuum filtered using 0.45 μm-pore filter paper (Whatman, Japan) prior to the acidification step. Shortly after the addition of HCl, sludge was formed on the surface of the solution. The acidification process was held until no further sludge was formed. The resulting sludge was removed by filtration and the filtrate was analyzed for COD using a spectrophotometer (HACH, DR3900, USA), and then used for the next procedure.

Based on the results, the filtrate from the optimum pH of acidification was further treated using various amounts of MgO powder (150, 300, 450, 600 and 750 mg L^{-1}). The MgO powder was added into the solution according to specific weights of separated beakers, stirred at 100 rpm for 30 min and left for 1 hr without stirring until the hydrogel was completely formed prior to the filtration using 0.45 μm-pore filter. The changing of pH was recorded. Filtrate from MgO pre-treatment was analyzed for COD and among the various weights of MgO used, the optimum weight was chosen. The selected filtrate was then treated using different amounts of geopolymer adsorbent (5, 7.5, 10, 12.5 and 15 mg L^{-1}) at 200 rpm using an incubated in orbital shaker (Lab Companion SIF6000R, Korea) at room temperature for predetermined times (1 to 24 hr). COD analysis was conducted to determine the effectiveness of the application of the sequential pre-treatment and geopolymer adsorbent. The summary of the overall batik wastewater sequential pre-treatment procedure was shown in Figure 1.
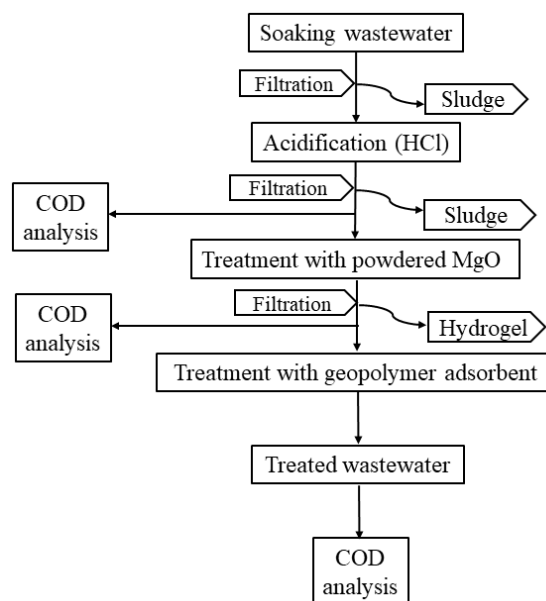
Figure1. The sequential pre-treatment of batik wastewater

RESULTS AND DISCUSSION

Characterization of geopolymer adsorbent

Surface area, pore volume, porosity and density analysis

The surface area, average pore diameter, pore volume, porosity and density of the GSA adsorbent was 12.8740

m^2 g^{-1}, 5.8675 nm, 1684.49 mm^3 g^{-1}, 87.64 % and 0.4930 g cm$^{3-1}$, respectively. Whereas, the surface area, average

pore diameter, pore volume, porosity and density of the geopolymer was 3.6113 m^2 g^{-1}, 3.3110 nm, 913.77 mm^3 g^{-1}, 20.81 % and 0.2195 g cm^{3-1}, respectively. The percentage of porosity reported in this work was considered high which surpassed a few types and shapes of the geopolymer adsorbent [26,27]. Obviously, the hybridization and addition of the egg white provided a great influence on the pore properties which contributed to the formation of high interconnected porosity geopolymer adsorbent. Both geopolymer and GSA adsorbent in Figure 2 exhibit Type IV isotherm which

suggested the occurrence of capillary condensation of the hysteresis loop of mesoporous materials [28]. The isotherm 'knee' of GSA adsorbent demonstrates increasing of N_2 volume adsorbed compared to the geopolymer which explained higher formation of pores in GSA adsorbent [29]. The GSA N_2 adsorption capacity was also higher about 15 cm^3 g^{-1} STP compared to the geopolymer adsorbent and this is the starting point of the multilayer coverage adsorption after completing the monolayer adsorption.
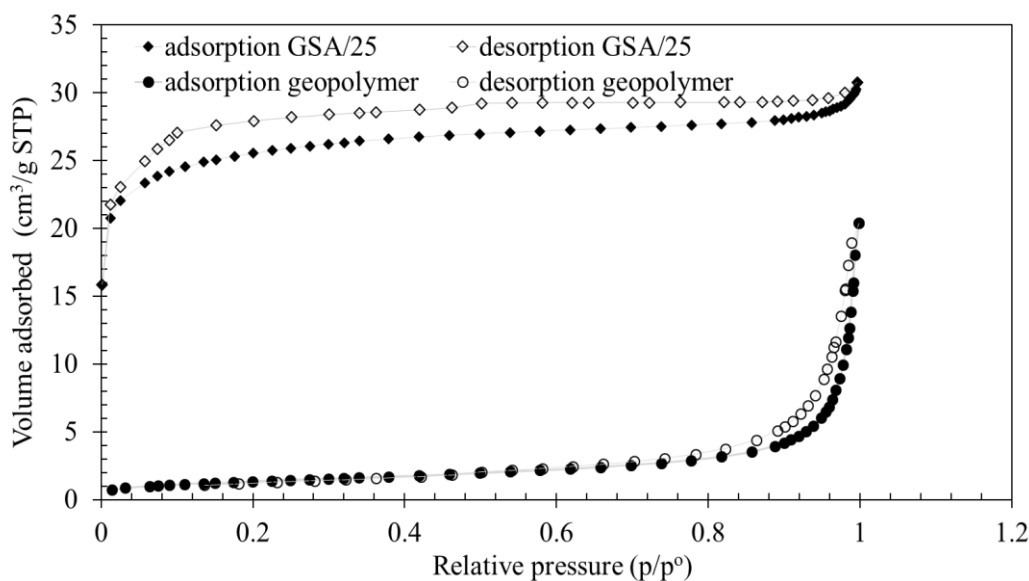
Figure 2. N_2 adsorption-desorption isotherms of geopolymer and GSA adsorbent

X-ray Diffraction Analysis

Figure 3 shows XRD spectra of the geopolymer and GSA adsorbent. Essentially, both results composed of amorphous phase and a few crystalline phases namely, quartz (SiO_2) (ICDD no.04-008-4821), calcite ($CaCO_3$) (ICDD no. 00-005-0586), mullite ($Al_6Si_2O_{16}$) (ICDD no. 05-001-0663) and Fe_2O_3 (ICDD no. 04-017-9123). Quartz was identified as the most intense phase in both samples. However, the intensities of all phases were remarkably dropped after the occurance of hybridization which was consistent with the findings' of other researchers[30]. The hump between 20° and 38° and centered at 27-29° corresponded to the presence of

amorphous inorganic aluminosilicates framework which associated with the occurance of the geopolymerization[31]. Only amorphous phase of the FA took part in the geopolymerization process while the crystalline phases such quartz, mullite and hematite were not fully reacted in the geopolymerization[32]. The incomplete geopolymerization process was due to the inadequate amount of NaOH used in the reaction as reported by other authors[21]. This broad peak was the major feature of XRD diffractogram of the geopolymer materials[21,33,34].
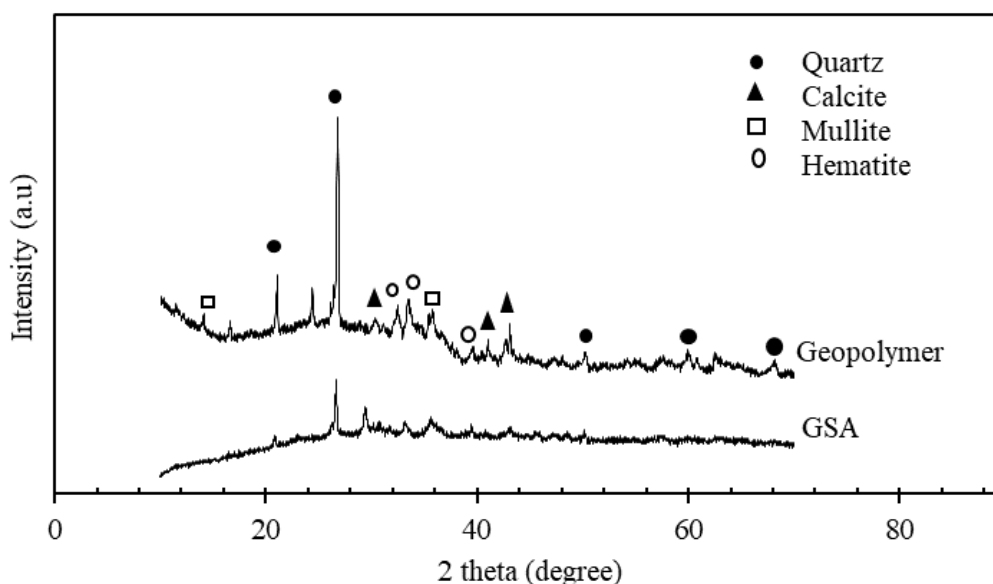
Figure 3. XRD diffractogram of the geopolymer and GSA adsorbent

Fourier transform infrared (FT-IR) spectroscopy Analysis

The FTIR spectrum of the SA, geopolymer and GSA adsorbent were illustrated in Figure 4. Both geopolymer and GSA spectra clearly showed the characteristic peaks of geopolymer existence and there was no significant difference between them.
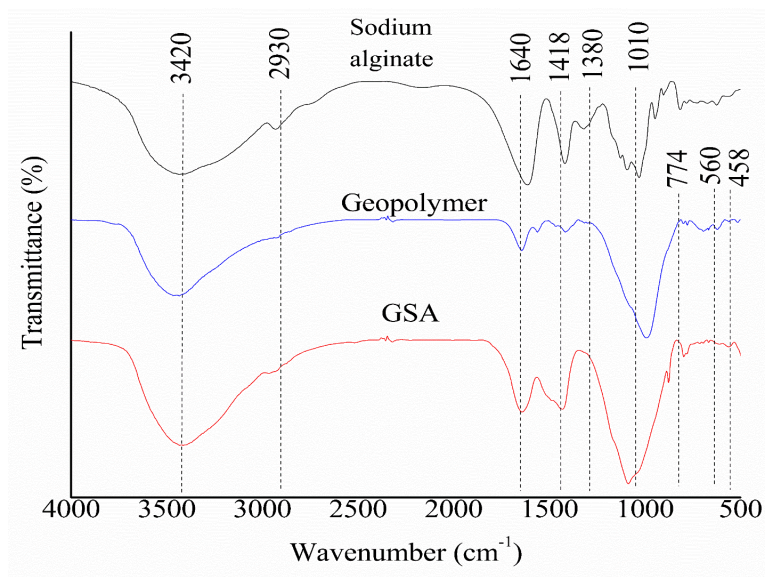
Figure 4. FTIR spectra of the geopolymer, SA and GSA adsorbent

In particular, the spectra presented broad absorption bands which associated with the amorphous characteristic of the geopolymer materials. The peaks at 458 and 560 cm^{-1} reffered to Si-O-Si bands and Si-O-Al bands, respectively. Furthermore, the band around 1010 cm^{-1} corresponded to the Si/Al-O-Si asymmetric stretching vibration, which over-lapped with the C-O-C stretching peak of SA[31]. The 774 cm^{-1} band related to Si-O-Si asymmetric stretching mode and the peaks around at 3420, 2930 and 1640 cm^{-1} attributed to O-H stretching of the silane groups and the remaining adsorbed water. The combination of C-OH deformation vibration and carboxylate symmetric stretch vibration was represented by the 1418 cm^{-1} peak. The bands around 1380 and 1010 cm^{-1} were contributed by the SA molecule that related to the asymmetric strecthing vibration bands of C-O-O. The

FTIR result of the GSA adsorbent strongly proved the structure composed of geopolymer and hybridized with SA.

Field Emission Scanning Electron Microscopy (FESEM) Imaging

Figure 5 shows the surface and cross-section microstructure of the geopolymer and GSA adsorbent at different magnifications, and also the EDS spectrum of both adsorbents. Remarkable differences between the adsorbents were observed that related to number, volume, size and distribution of the pores. The GSA adsorbent (Figure 5(d)-(f)) exhibited good spherical shape with homogeneous and smooth surface and very porous structure which was in agreement with surface area, pore volume and porosity analysis results. Whereas, fewer number, volume, size and distribution of pores were shown for the geopolymer adsorbent. Several small pores on the surface of the GSA adsorbent allowed the MB

diffusion onto the adsorbent, thus ameliorated the adsorption capacity of the adsorbent. Figure 5 (e) shows the adsorbent was distinctly porous with honeycomb network microstructure, in which most of the pores were connected pores and uneven pore size distribution. Several small-sized open pores were also clearly visible inside the larger-sized closed pore. This condition enhanced the number of active sites available for the adsorption of MB. FESEM micrographs (Figure 5) demonstrated the hybridization and addition of egg white as the foaming agent evidently changed the microstructure of the adsorbent which made it feasible for the application as an adsorbent. The EDS spectrum results suggested that both adsorbent contained similar composition of Si, Al, Na, Mg, Fe and Ca. The presence of Cl element was observed for GSA EDS spectrum reflecting from immersion in $CaCl_2$ during the preparation of the adsorbent.
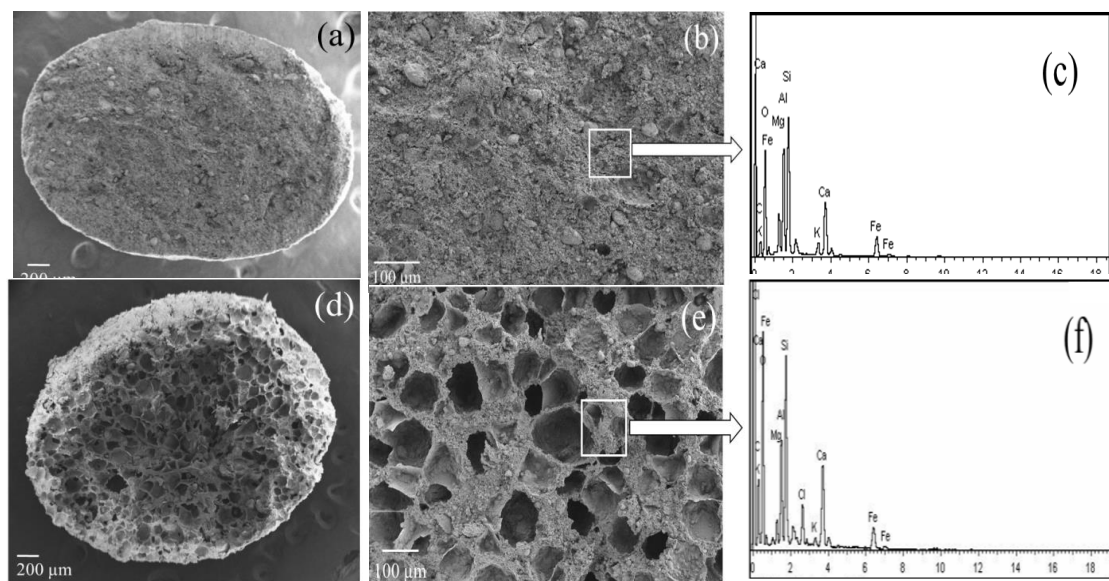
Figure 5. FESEM micrographs of surface appearance and cross-section of geopolmer ((a)-(c)) and GSA ((d)-(f))

Characterization of batik wastewater

The characteristic results of the batik wastewater is summarized in Table 1. On the basis of the characterization, the batik wastewater can be considered as high strength batik wastewater due to the high values of COD, ADMI colour intensity, TSS and turbidity[14] which is significantly higher than the standard limit

regulated by Department of Environment (DOE) Malaysia, EQA 1974, for Environmental Quality (Industrial Effluents) Regulation 2009 of the Fifth Schedule for Standards A and B[35], and the Seventh Schedule (Regulation 12) for COD[6].

Table 1. Main characteristics of the untreated batik wastewater

Parameter	Value
COD	4113 mg/L
Colour (ADMI)	1100
Turbidity	26.30± 0.2 ntu
TSS	32.5 mg/L
pH	11.2

The sludge started to form instantly at pH 3.50 when the batik wastewater was under the acidification using concentrated HCl and more flocs was appeared on the surface of the batik wastewater when pH reached to lower values of 1-3. Prior to the acidification, the COD concentration was 4113 mg L^{-1} and after treating at pH 1, 2 and 3 by the concentrated HCl, it was decreased to 1089, 535 and 287 mg L^{-1}, respectively (Figure 6(a)). In the acidification stage, the sodium silicate in the batik wastewater was dissolved and formed a negatively soluble silicate species and at lowered pH, the silicate was converted to silicic acid. A dimer silicate was yielded from the reaction of two silicic acid, which further polymerized and resulted in polymerized SiO_2. Then, these polymerized SiO_2 were coordinated with the typical wax ester of the batik wastewater through a coordination of oxygen molecule of the waxes with the silano grous (Si-OH) by the hydrogen bonding. The waxes composed of long alkyl chains which consisted of fatty acids and primary alcohols[14]. In term of COD removal, the percentage was increased from 73.5- 93%, with the increment of pH from 1 to 3. Thus, it was concluded that the significant reduction of COD concentration was occured at pH 3 which resulted in the maximum removal of this stage. This acidic effluent was filtered and used for the subsequent treatment using MgO powder.

Various amounts of MgO (150 – 750 mg L^{-1}) were utilized in the pre-treatment by the MgO powder. Figure 6(b) and Figure 7 depicted the changes of COD concentration and pH, respectively with the addition of MgO to the effluent after the subjection to the acidification stage. Figure 6(b) shows the COD concentration was gradually decreased from 287 mg/L to 209 mg L^{-1} over the different amounts of MgO powder addition. In the MgO pre-treatment the main constituent of COD, waxes and dyes were incorporated with the solid complex in the effluent [1]. Hydrogels were started to form after ~20 min with addition of MgO powder. Furthermore, the removal percentage of the COD was also increased from 4 – 27%. The pre-treatment using MgO powder did not only significantly reduce the COD concentration, but also changed the pH of the effluent which gradually increased from pH 3 to 8.75, over the entire range of MgO amounts (Figure 7). In this stage, the MgO was hydrolyzed to $Mg(OH)_2$ in the presence of water. Next, the $Mg(OH)_2$ was dissociated to hydroxyl ions (OH^-) which increased the pH of the effluent. This reaction also hydrolyzed and precipitated most of the heavy metals that presented in the effluent.
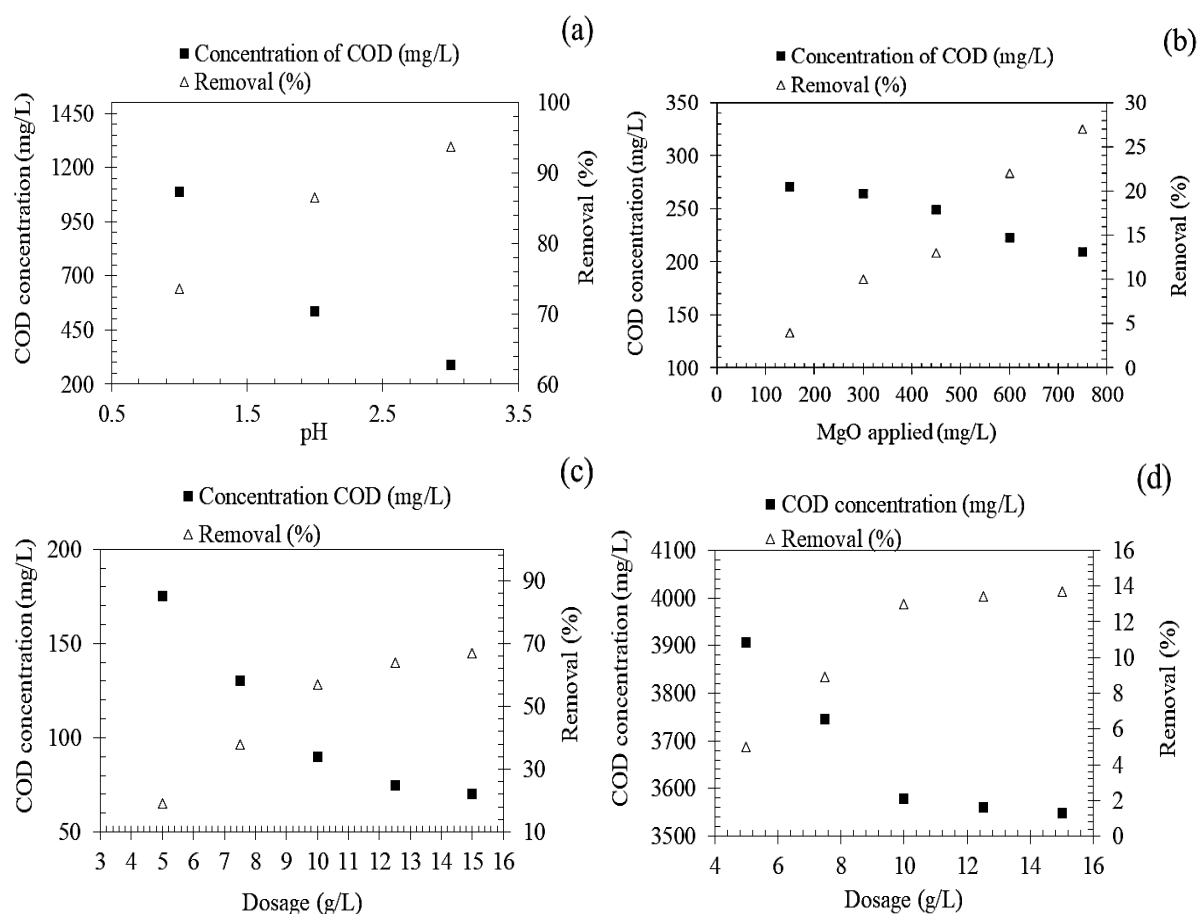
Figure 6. COD concentration (mg/L) and its removal efficacy (%) (a) after acidification, (b) after application of MgO powder, (c) after treating with GSA and subjected to sequential pre-treatment before the adsorption process and (d) after treating with GSA adsorbent without sequential pre-treatment

The hydrogel that was formed during the pre-treatment by MgO considerably removed the significant amount of polymerized organic compund as the COD concentration was reduced from 287 mg L^{-1} to 209 mg L^{-1} over the entire range amount of MgO. Thus, at this stage, the dyes were left as the main organic pollutant and remained in the effluent. Figure 6(c) and 6(d) shows the COD concentration and removal for batik wastewater after subjected to the treatment by the geopolymer adsorbent with and without application of sequential pre-treatment, respectively. Figure 6(c) exhibits the geopolymer adsorbent successfully reduced the COD concentration (175 – 70 mg L^{-1}) to the content which met the Seventh Schedule (Regulation 12) of COD [6], for the application of adsorbent as low as 10 g L^{-1}. Meanwhile, the COD

removal percentage was increased from 19 - 67% over the entire range of the dosage applied in the adsorption. The COD concentration of batik wastewater that was not subjected to the sequential pre-treatment before adsorption by the adsorbent was not significantly decreased (3907 – 3549 mg L^{-1}) for any amount of adsorbent used and the values were still too high to comply with the Seventh Schedule (Regulation 12) of COD[6]. Thus, it can be concluded that the batik wastewater treatment must undergo the sequential pre-treatment prior to the adsorption by the geopolymer adsorbents which can remove the silicates, waxes and heavy metals in the water that resulted the unsuccessful reduction of COD concentration.

353
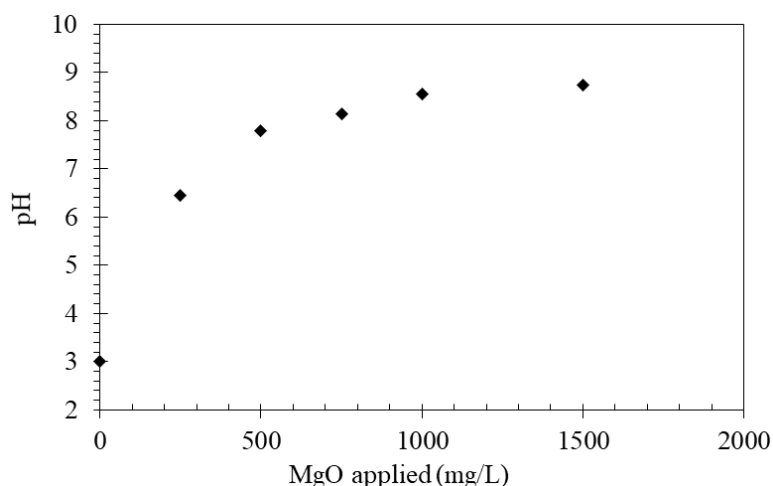
Figure 7. The changing of pH according to MgO application

CONCLUSIONS

In this investigation, high porosity hybrid geopolymer / sodium alginate (GSA) adsorbent was prepared and used to remove dyes from wastewater. A sequential pre-teatment that involved acidification using high concentrated HCl followed by pre-treatment using MgO powder and finally adsorption by high porosity hybrid fly ash geopolymer adsorbent spheres were applied to treat batik wastewater which heavily polluted with silicates, dyes and heavy metals. In the acidification stage, ~73.5-93% of the COD was removed through the increment of pH from 1 to 3. In the next stage, removal percentage of the COD was also increased from 4 – 27% over the entire range of MgO amounts of 150 to 750 mg L^{-1}. Finally, the adsorption by the GSA adsorbent successfully reduced the COD concentration (175 – 70 mg L^{-1}) to the content which met the Seventh Schedule (Regulation 12) of COD for the application of adsorbent as low as 10 g L^{-1}. According to the current findings, this 2-stage treatment that involved acidification and pre-treatment with MgO prior to adsorption by geopolymer adsorbent can be considered as feasible, economical and effective sequential pre-treatment for the treatment of batik wastewater.

ACKNOWLEDGEMENTS

Conflict of interests

No conflict.

REFERENCES

1.Desa A.L., Hairom N.H.H., Ng L.Y., Ng C.Y., Ahmad M.K., Mohammad A.W., 2019. Industrial Textile Wastewater Treatment Via Membrane Photocatalytic Reactor (MPR) In The Presence of Zno-PEG Nanoparticles and Tight Ultrafiltration. Journal of Water Process Engineering. 31, 100872.

2. Pang Y.L., Abdullah A.Z., 2013. Current Status of Textile Industry Wastewater Management And Research Progress In Malaysia: A Review. CLEAN - Soil, Air, Water. 41(8), 751-764.

3. Rashidi H., Nik Sulaiman N.M., Awanis Hashim N., Che Hassan C.R., Davazdah Emami S., 2015. Simulated Textile (Batik) Wastewater Pre-Treatment Through Application Of A Baffle Separation Tank. Desalination and Water Treatment. 57(1), 151-160.

4. Effendi H., Sari R., Hasibuan S., 2020. In 35 th Annual Conference of the International Association for Impact Assessment, AIA15 Conference Proceedings: Florence-Italy, October.

5. Natarajan T.S., Natarajan K., Bajaj H.C., Tayade R.J., 2013. Study on Identification of Leather Industry Wastewater Constituents and Its Photocatalytic Treatment. International Journal of Environmental Science and Technology. 10(4), 855-864.

6. Khalik W.F.W.M., Ho L.N., Ong S.A., Wong Y.S., Yusoff N.A., Ridwan F., 2015. Decolorization and

Mineralization Of Batik Wastewater Through Solar Photocatalytic Process. Sains Malaysiana. 44(4), 607-612.

7. Mukimin A., Vistanty H., Zen N., Purwanto A., Wicaksono K.A., 2018. Performance of Bioequalization-Electrocatalytic Integrated Method for Pollutants Removal of Hand-Drawn Batik Wastewater. Journal of Water Process Engineering. 21, 77-83.

8. Suteu D., Zaharia C., Măluțan T., 2012. Biosorbents Based on Lignin Used in Biosorption Processes from Wastewater Treatment: A Review, 1st ed., Nova Science Publishers Inc.: New York. pp 279-305.

9. Sutisna, Wibowo E., Rokhmat M., Rahman D.Y., Murniati R., Khairurrijal, Abdullah M., 2017. Batik Wastewater Treatment Using TiO_2 Nanoparticles Coated on the Surface of Plastic Sheet. Procedia Engineering. 170, 78-83.

10. Natarajan S., Bajaj H.C., Tayade R.J., 2018. Recent Advances Based on The Synergetic Effect of Adsorption for Removal of Dyes from Waste Water Using Photocatalytic Process. Journal of Environmental Sciences. 65, 201-222.

11. Barbosa T.R., Foletto E.L., Dotto G.L., Jahn S.L., 2017. Preparation of Mesoporous Geopolymer Using Metakaolin And Rice Husk Ash As Synthesis Precursors And Its Use As Potential Adsorbent To Remove organic Dye From Aqueous Solutions. Ceramics International. 44(1), 416-423.

12. Novais R.M., Ascensão G.A., Tobaldi D.M., Seabra M.P., Labrincha J.A., 2018. Biomass Fly Ash Geopolymer Monoliths For Effective Methylene Blue Removal From Wastewaters. Journal of Cleaner Production. 171, 783-794.

13. Novais R.M., Carvalheiras J., Tobaldi D.M., Seabra M.P., Pullar R.C., Labrincha J.A., 2019 Synthesis of Porous Biomass Fly Ash-Based Geopolymer Spheres For Efficient Removal Of Methylene Blue From Wastewaters. Journal of Cleaner Production. 207, 350-362.

14. Birgani P.M., Ranjbar N., Che Abdullah R., Wong K.T., Lee G., Ibrahim S., Park C., Yoon Y., Jang M., 2016. An Efficient and Economical Treatment for Batik Textile Wastewater Containing High Levels of Silicate and Organic Pollutants Using A Sequential Process Of Acidification, Magnesium Oxide, And Palm Shell-Based

Activated Carbon Application. Journal of Environmental Management. 184, 229-239.

15. Lau W.J., Ismail A.F., 2009. Polymeric Nanofiltration Membranes For Textile Dye Wastewater Treatment: Preparation, Performance Evaluation, Transport Modelling, and Fouling Control — A Review. Desalination. 245(1-3), 321-348.

16. Harif T., Khai M., Adin A., 2012. Electrocoagulation Versus Chemical Coagulation: Coagulation / Flocculation Mechanisms And Resulting Floc Characteristics. Water Research. 46(10), 3177-3188.

17. Cardoso J.C., Bessegato G., Boldrin Zanoni M.V., 2016. Efficiency Comparison of Ozonation, Photolysis, Photocatalysis and Photoelectrocatalysis Methods In Real Textile Wastewater Decolorization. Water Research. 98, 39-46.

18. Soni H., Nirmal Kumar J.I., Patel K., Kumar R.N., 2015. Photocatalytic Decoloration of Three Commercial Dyes In Aqueous Phase And Industrial Effluents Using TiO_2nanoparticles. Desalination and Water Treatment. 57(14), 6355-6364.

19. Souza R.P., Freitas T.K.F.S., Domingues F.S., Pezoti O., Ambrosio E., Ferrari-Lima A.M., Garcia J.C., 2016. Photocatalytic Activity Of Tio2, Zno And Nb2o5 Applied To Degradation Of Textile Wastewater. Journal of Photochemistry and Photobiology A: Chemistry. 329, 9-17.

20. Tong D.S., Wu C.W., Adebajo M., Jin G.C., Yu W.H., Ji S.F., Zhou C.H., 2018. Adsorption of Methylene Blue From Aqueous Solution Onto Porous Cellulose-Derived Carbon / Montmorillonite Nanocomposites. Applied Clay Science. 161, 256-264.

21. Khan M.I., Min T.K., Azizli K., Sufian S., Ullah H., Man Z., 2015. Effective Removal of Methylene Blue From Water Using Phosphoric Acid Based Geopolymers: Synthesis, Characterizations And Adsorption Studies. RSC Advances. 5(75), 61410-61420.

22. Boca Santa R.A.A., Kessler J.C., Soares C., Riella H.G., 2018. Microstructural Evaluation of Initial Dissolution of Aluminosilicate Particles And Formation Of Geopolymer Material. Particuology. 41, 101-111.

23. Ahmaruzzaman M., 2011. Industrial Wastes As Low-Cost Potential Adsorbents For The Treatment of Wastewater Laden With Heavy Metals. Advances in Colloid and Interface Science. 166(1-2), 36-59.

24. Pawar R.R., Lalhmunsiama L., Gupta P., Sawant S.Y., Shahmoradi B., Lee S., 2018. Porous Synthetic Hectorite Clay-Alginate Composite Beads For Effective Adsorption of Methylene Blue Dye From Aqueous Solution. International Journal of Biological Macromolecules. 114, 1315-1324.

25. Hussein Safauldeen S., Abu Hasan H., Sheikh Abdullah S.R., 2019. Phytoremediation Efficiency Of Water Hyacinth For Batik Textile Effluent Treatment. Journal of Ecological Engineering. 20(9), 177-187.

26. Bai C., Colombo P., 2016. High-Porosity Geopolymer Membrane Supports By Peroxide Route With The Addition Of Egg White As Surfactant. Ceramics International. 43(2), 2267-2273.

27. Xu F., Gu G., Zhang W., Wang H., Huang X., Zhu J., 2018. Pore Structure Analysis and Properties Evaluations of Fly Ash-Based Geopolymer Foams By Chemical Foaming Method. Ceramics International. 44(16), 19989-19997.

28. Yahia M.B., Torkia Y.B., Knani S., Hachicha M.A., Khalfaoui M., Lamine A.B., 2013. Models For Type VI Adsorption Isotherms From A Statistical Mechanical Formulation. Adsorption Science & Technology. 31(4), 341-357.

29. Saafie N., Samsudin M.F.R., Sufian S., Ramli R.M., 2019. Enhancement of The Activated Carbon Over Methylene Blue Removal Efficiency Via Alkali-Acid Treatment. Proceeding of the 6th International Conference on Environment (ICENV2018): Empowering Environment and Sustainable Engineering Nexus Through Green Technology, Penang, December 11-13.

30. Ge Y., Cui X., Kong Y., Li Z., He Y., Zhou Q., 2014. Porous Geopolymeric Spheres For Removal of Cu(II) From Aqueous Solution: Synthesis And Evaluation. Journal of Hazardous Materials. 283, 244-251.

31. Firdous R., Stephan D., Djobo J.N.Y., 2018. Natural Pozzolan Based Geopolymers: A Review on Mechanical, Microstructural and Durability Characteristics. Construction and Building Materials. 190, 1251-1263.

32. Nath S., Kumar S., 2019. Reaction Kinetics of Fly Ash Geopolymerization: Role of Particle Size Controlled By Using Ball Mill. Advanced Powder Technology. 30(5), 1079-1088.

33. Maleki A., Mohammad M., Emdadi Z., Asim N., Azizi M., Safaei J., 2018. Adsorbent Materials Based on A Geopolymer Paste for Dye Removal From Aqueous Solutions. Arabian Journal of Chemistry. 13(1), 3017-3025.

34. Siyal A.A., Shamsuddin M.R,, Rabat N.E., Zulfiqar M.T., Man Z., Low A., 2019. Fly Ash Based Geopolymer For The Adsorption of Anionic Surfactant From Aqueous Solution. Journal of Cleaner Production. 229, 232-243.

35. Department of Environment. Environmental Requirements: A Guide For Investors. Ministry of Natural Resources and Environment. 2010, (October), 1–78.